

# Reduction and Functionalization of Graphene Oxide Sheets Using Biomimetic Dopamine Derivatives in One Step

Izabela Kaminska,<sup>†,‡</sup> Manash R. Das,<sup>§</sup> Yannick Coffinier,<sup>†</sup> Joanna Niedziolka-Jonsson,<sup>‡</sup> Jonusz Sobczak,<sup>‡</sup> Patrice Woisel,<sup>||</sup> Joel Lyskawa,<sup>||</sup> Marcin Opallo,<sup>‡</sup> Rabah Boukherroub,<sup>†,\*</sup> and Sabine Szunerits<sup>†,\*</sup>

<sup>†</sup>Institut de Recherche Interdisciplinaire (IRI), CNRS USR 3078, Université de Lille1, Parc de la Haute Borne, 50 avenue de Halley, BP 70478, 59658 Villeneuve d'Ascq Cedex, France

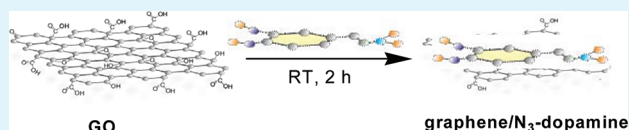
<sup>‡</sup>Institute of Physical Chemistry, Polish Academy of Sciences, Kasprzaka 44/52, 01-224 Warszawa, Poland

<sup>§</sup>Materials Science Division, North East Institute of Science and Technology (NEIST), CSIR, Jorhat 785006, Assam, India

<sup>||</sup>U STL, Unité des Matériaux Et Transformations (UMET, UMR 8207), Equipe Ingénierie des Systèmes polymères (ISP), F-59655 Villeneuve d'Ascq Cedex, France

**ABSTRACT:** An easy and environmentally friendly chemical method for the simultaneous reduction and noncovalent functionalization of graphene oxide (GO) using dopamine derivatives is described. The reaction takes place at room temperature under ultrasonication of an aqueous suspension of GO and a dopamine derivative. X-ray photoelectron spectroscopy, FT-IR spectroscopy, and cyclic voltammetry characterizations revealed that the resulting material consists of graphene functionalized with the dopamine derivative. This one-step protocol is applied for simultaneous reduction and functionalization of graphene oxide with a dopamine derivative bearing an azide function. The chemical reactivity of the azide function was demonstrated by a postfunctionalization with ethynylferrocene using the Cu(I) catalyzed 1,3-dipolar cycloaddition.

**KEYWORDS:** graphene, dopamine, reduction, click chemistry, electrochemistry, azide function



## 1. INTRODUCTION

Graphene has shown great promise for applications in different areas such as electronics, energy storage, and conversion as well as in the development of biosensors.<sup>1–6</sup> Different methods have been reported for the preparation of high-quality graphene such as chemical vapor deposition (CVD) on metal or silicon substrates and mechanical exfoliation using strong oxidants.<sup>1,7</sup> The exfoliated sheets are distorted carbon networks carrying carboxylate, hydroxyl, and other oxygen containing functional groups commonly referred to as graphene oxide (GO). While these functional groups enable the suspension of GO sheets in water and other polar solvents, their sp<sup>2</sup> network is partially destroyed. As a consequence, GO sheets display an electrical insulating character. Reduction of GO with hydrazine hydrate is commonly used to restore the sp<sup>2</sup> structure.<sup>8</sup> However, hydrazine hydrate is a strong and highly poisonous reducing agent. Therefore, recently great efforts have been devoted to explore milder reduction methods and to improve the stability and dispersity of graphene in water.<sup>9</sup> On the other hand, chemical modification plays an important role in improving and manipulating the properties of graphene for its effective usage in various applications.<sup>10–12</sup> Next to covalent modification,<sup>10–12</sup> the noncovalent functionalization involving strong  $\pi$ - $\pi$  interactions between the graphene sheets and aromatic molecules has been investigated more recently.<sup>11,13–17</sup> Pyrene and pyrene derivatives<sup>13–15</sup> have been used next to polydopamine,<sup>18</sup> and electron acceptors and donors such as tetrathiafulvalene (TTF), tetracyanethylene, or 3-dichloro-5,6-

dicyano-1,4-benzo-quinone<sup>16,17</sup> to modify graphene nano-sheets. Dopamine, chemically known as 3,4-dihydroxy-L-phenylalanine and one of the crucial catecholamine neurotransmitters widely distributed in mammalian brain tissues, is particularly interesting for its strong interaction with metal oxides<sup>19–21</sup> and graphene.<sup>18,22–24</sup> The interest in using dopamine as a moiety is the ease with which functional groups like azide and others can be introduced via its amine groups. This also limits its self-polymerization process forming polydopamine at weak alkaline pH.

We report here on an interesting strategy allowing simultaneous reduction of GO to graphene and its functionalization with azide-terminated dopamine. The azide function of the resulting graphene/dopamine composite films allowed in a follow up step the use of the copper(I)-catalyzed 1,3-dipolar cycloaddition to “click” alkyne-terminated molecules to the interface. The concept of “click” chemistry, introduced by Sharpless and based on the triazole ring formation between azides and alkynes, is particularly well-suited for this purpose due to the use of mild reaction conditions and its high reaction efficiency.<sup>11,25–27</sup> In a proof of concept experiment, ethynylferrocene was linked to N<sub>3</sub>-functional graphene composite films (Figure 1).

**Received:** November 28, 2011

**Accepted:** January 3, 2012

**Published:** January 3, 2012

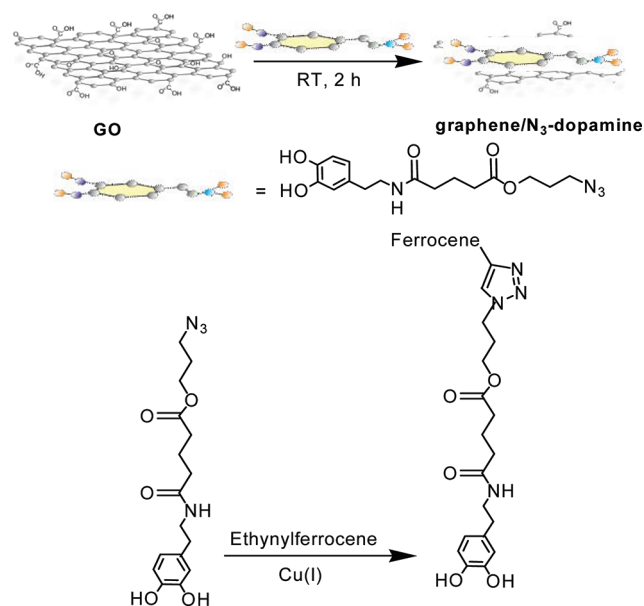


**Figure 1.** Schematic illustration of the preparation of azido-dopamine capped graphene nanosheets and “click” chemistry.

## 2. EXPERIMENTAL SECTION

**2.1. Materials.** Graphite powder (<20  $\mu\text{m}$ ), dimethylsulfoxide (DMSO), potassium chloride (KCl), ethynylferrocene, CuI, triethylamine (TEA), ruthenium hexamine trichloride ( $\text{Ru}(\text{NH}_3)_6\text{Cl}_3$ ), and tin-doped indium oxide coated glass (ITO) (sheet resistivity 15–25  $\Omega\text{-cm}^2$ ) were purchased from Aldrich and used as received.

The azide-terminated dopamine anchor was prepared as previously described.<sup>21</sup>

**2.2. Preparation of Graphene Oxide (GO).** Graphene oxide (GO) was synthesized from graphite powder by a modified Hummers method.<sup>28</sup> A total of 0.5 mg of the synthesized graphite oxide was dispersed in 100 mL of water, exfoliated through ultrasonication for 3 h, and used as a stock of GO–water suspension.

**2.3. Preparation of Graphene/Azide-Terminated Dopamine.** The initial graphene oxide (GO) solution was diluted in 1 mL of water (1:10). A total of 1 mL of azide-terminated dopamine (10 mM) was added to 1 mL of GO, and the mixture was left for 1 h in an ultrasonic bath. A precipitate was formed and separated from the aqueous supernatant by centrifugation at 14 000 rpm for 20 min.

**2.4. “Click” Reaction on Graphene/Azide-Terminated Dopamine.** Graphene/azide-terminated dopamine modified ITO electrodes were prepared by casting 50  $\mu\text{L}$  of graphene/dopamine water solution onto the ITO electrode and left for evaporation. In the latter step the “click” reaction between the azide-terminated surface with alkynyl-terminated ferrocene was performed. Ethynylferrocene (2 mM), CuI (3.15 mM), and TEA (43 mM) were added into  $\text{CH}_3\text{CN}$  (10 mL).<sup>29</sup> Previously prepared substrates were immersed into the solution and stirred for 24 h at room temperature.

**2.5. Characterization.** X-ray photoelectron spectroscopy (XPS) experiments were performed in a PHI 5000 VersaProbe-Scanning ESCA Microprobe (ULVAC-PHI, Japan/USA) instrument at a base pressure below  $5 \times 10^{-9}$  mbar. Monochromatic  $\text{AlK}_\alpha$  radiation was used and the X-ray beam, focused to a diameter of 100 micrometer, was scanned on a  $250 \times 250$  micrometer surface, at an operating power of 25 W (15 kV). Photoelectron survey spectra were acquired using a hemispherical analyser at pass energy 117.4 eV with a 0.4 eV energy step, core-level spectra were acquired at pass energy 23.5 eV with a 0.1 eV energy step. All spectra were acquired with  $90^\circ$  between X-ray source and analyser and with the use of low energy electrons and low energy argon ions for charge neutralization. After subtraction of the Shirley-type background, the core-level spectra were decomposed into their components with mixed Gaussian-Lorentzian (30:70) shape

lines using the CasaXPS software. Quantification calculations were conducted with using sensitivity factors supplied by PHI.

FTIR spectra were recorded using an IRAffinity-1 Fourier Transform Infrared Spectrophotometer (SHIMADZU Co-operation, Japan) at  $4 \text{ cm}^{-1}$  spectral resolution. The samples were prepared by casting 50  $\mu\text{L}$  of graphene oxide or graphene/dopamine composite materials on a silicon wafer heated at  $70^\circ\text{C}$ . The samples were mounted in a purged sample chamber. Background spectra were obtained using a flat untreated Si(100).

Cyclic voltammetry experiments were performed using an Autolab 20 potentiostat (Eco Chimie, Utrecht, The Netherlands). The electrochemical cell consisted of a working electrode (ITO or modified ITO), Ag/AgCl (Bioanalytical Systems, Inc.) as reference electrode, and platinum wire as counter electrode. Cyclic voltammetric measurements were performed in 10 mM  $\text{Ru}(\text{NH}_3)_6\text{Cl}_3$  in KCl (0.1 M) at a scan rate  $\nu = 0.05 \text{ V s}^{-1}$ .

Graphene oxide and graphene/azide-terminated dopamine modified ITO electrodes were prepared by casting 50  $\mu\text{L}$  of an aqueous solution of graphene oxide onto the ITO substrate heated at  $70^\circ\text{C}$ .

## 3. RESULTS AND DISCUSSION

The interest of using dopamine in combination with graphene oxide is based on the physicochemical properties of dopamine.<sup>30</sup> Dopamine has been shown to be a good reducing agent for metallic salts such as  $\text{HAuCl}_4$  or  $\text{H}_2\text{PtCl}_6$ .<sup>30,31</sup> In parallel, the fascinating adhesion and self-polymerization properties at weak alkaline pH has made dopamine interesting as a capping agent. This allows dopamine to be used for a one-step reaction whereby GO is reduced and decorated with dopamine at the same time. Motivated by the mild conditions used in “click” chemistry, azide-terminated dopamine ( $\text{N}_3$ -dopamine) was investigated here.  $\text{N}_3$ -dopamine modified graphene was obtained by simply mixing an aqueous solution of GO with the dopamine derivative under sonication at room temperature. After 1 h of reaction, a precipitate, dissoluble in DMSO and DMF but nondispersible in polar solvents, was formed that could be separated from the supernatant aqueous solution by centrifugation. The interaction between dopamine and graphene is most likely dominated by  $\pi$ -stacking between the hexagonal cells of graphene and the aromatic ring structure of dopamine. However, as the  $\text{N}_3$ -dopamine acts as reducing agent, the graphene oxide is likely to oxidize the ortho-quinol structure of the  $\text{N}_3$ -dopamine to radical or quinone intermediates which are likely to covalently bind to graphene or to each other.

The chemically exfoliated GO contains a variety of functional groups such as hydroxyl (C–OH), epoxide (C–O–C), carbonyl (C=O), and carboxyl (COOH) groups usually present at the defects and edges of the sheets. X-ray photoelectron spectroscopy (XPS) analysis was performed on GO before and after reaction with dopamine derivatives to gain further information on its chemical composition. The C 1s core level spectrum of GO nanosheets is shown in Figure 2A and can be deconvoluted into four peak components with binding energies at about 283.8, 284.7, 286.7, and 287.9 eV assigned to  $\text{sp}^2$ -hybridized carbon,  $\text{sp}^3$ -hybridized carbon, C–O and C=O species, respectively. GO can be obtained with a range of C/O stoichiometries depending on the details of the particular synthesis. The C/O ratio of GO is 1.73, comparable to reported data.<sup>32,33</sup>

Figure 2B displays the C 1s XPS spectrum of the resulting graphene/dopamine- $\text{N}_3$  composite material. The intensity of the  $\text{sp}^2$ -hybridized carbon at 283.8 eV became predominant. Additional bands at 284.9, 286.8, and 287.9 eV are also observed and can be attributed to C–C/C–H, C–O/C–N,

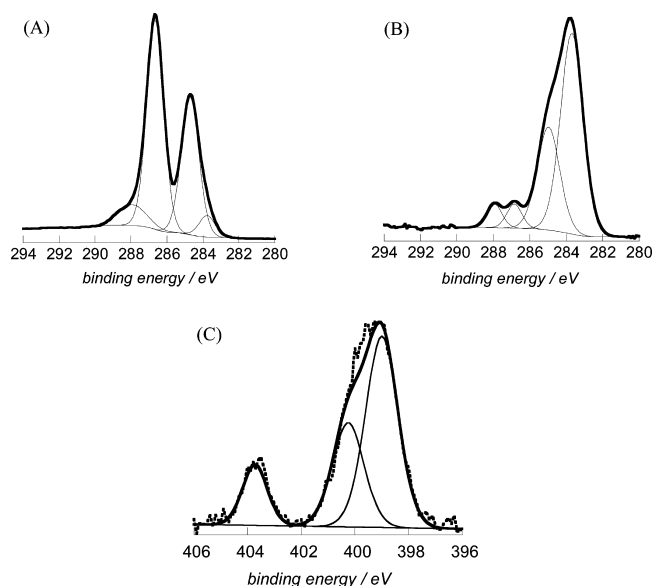


**Figure 2.** C 1s core-level XPS spectra of GO before (A) and after reaction with dopamine- $N_3$  (B); (C) N 1s core level spectrum of graphene/dopamine- $N_3$  composite material.

and C=O, respectively. The ratio of carbon to oxygen is increased to about 3.4. This is comparable to photochemically reduced GO ( $C/O = 3.3$ )<sup>33</sup> but lower than that reported by Stankovich et al. for hydrazine-reduced GO with  $C/O = 10.3$ .<sup>34</sup> However, the reduction process was accompanied by nitrogen incorporation with a ratio of  $C/N = 16.1$ , which results in  $C/(O + N) = 6$ .<sup>34</sup> The presence of a band at 400 eV due to N 1s (Figure 2C) suggests the incorporation of azide-terminated dopamine in the reduced graphene nanosheets. It can be deconvoluted into three peaks at 398.9 ( $NH_2$  and  $N=N=N$ ), 400.3 ( $NH-C=O$ ), and 403.7 eV ( $N=N=N$ ), consistent with the chemical composition of the dopamine derivative (Figure 1).<sup>35–37</sup>

To understand the influence of the  $N_3$  function in dopamine on GO reduction, a similar experiment was carried out with unmodified dopamine. The determined C/O ratio is about 3.8, slightly higher than in the case of  $N_3$ -dopamine. However, the presence of O—C=O and N—C=O bonds in the synthetic  $N_3$ -dopamine (Figure 1) is also responsible for the lower C/O ratio of graphene/ $N_3$ -dopamine composite films compared to graphene/dopamine ones. It thus seems that the influence of the  $N_3$  function is neglectable.

The success of the incorporation of azide-terminated dopamine in the reduced graphene nanosheets was additionally confirmed by FTIR spectroscopy. The FTIR spectrum of graphene oxide deposited onto silicon substrate by drop casting is displayed in Figure 3A. It is dominated by a broad band at  $3250\text{ cm}^{-1}$  assigned to the vibration of surface hydroxyl groups and/or adsorbed water molecules. Furthermore, bands due to C=O (—COOH) vibration, OH deformation, and C—O (alkoxy) and C—O (epoxy) stretching modes are visible at 1729, 1425, 1237, and  $1063\text{ cm}^{-1}$ , respectively. The results are in accordance with the XPS data, suggesting the presence of various carbon–oxygen related groups on GO surface. The band at  $1590\text{ cm}^{-1}$  can be attributed to aromatic C=C double bond stretching and C—H bending vibration frequencies of the carbon network. After reaction of graphene oxide with azide-terminated dopamine (Figure 3B), a strong vibration band at  $2103\text{ cm}^{-1}$  characteristic of the asymmetric  $N_3$  stretching mode

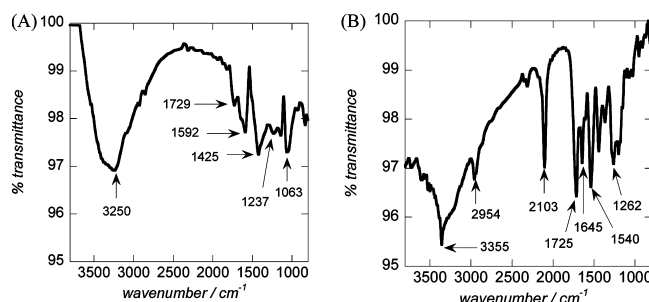


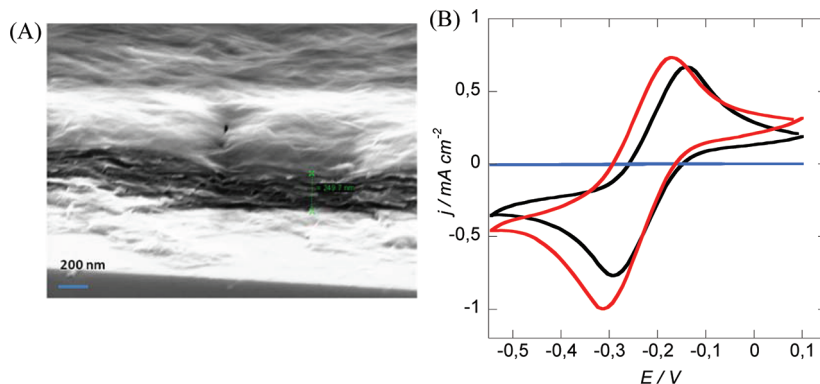
**Figure 3.** FTIR spectra of graphene oxide before (A) and after reaction with dopamine- $N_3$  (B).

appears.<sup>29</sup> In addition, bands at 1645 and  $1546\text{ cm}^{-1}$  corresponding to amide (I) and amide (II) vibrations and  $1725\text{ cm}^{-1}$  due to C=O of the dopamine conjugate are observed. The results are consistent with the chemical insertion of dopamine- $N_3$  within the graphene sheets. It is also to be noted that the band at  $3250\text{ cm}^{-1}$  in GO is significantly reduced, suggesting the reduction of GO.

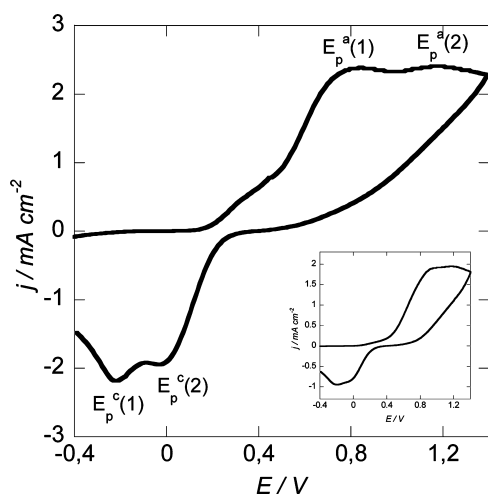
Electrochemical measurements were performed to characterize the electrical properties of graphene/dopamine- $N_3$  composite material. The drop casting process is very reproducible and leads to homogeneous distribution of GO and graphene/dopamine- $N_3$  flakes on the ITO interface with film thicknesses of  $\sim 44\text{ nm}$  (GO) and  $\sim 250\text{ nm}$  (graphene/dopamine- $N_3$ ) (Figure 4A). Figure 4B shows cyclic voltammograms (CV) of a bare ITO before and after drop casting a film of GO and graphene/dopamine- $N_3$  in  $Ru(NH_3)_6^{3+/2+}$ . It is well-known that  $Ru(NH_3)_6$  is behaving like an outer-sphere redox system that is relatively insensitive to surface microstructures, surface oxides, and impurities.<sup>38,39</sup> The electronic properties of the electrode, especially the density of electronic states near the formal potential of the redox system, is the most important factor affecting the reaction rate. The results show that the detected current densities of reduced graphene/dopamine- $N_3$  exceeds that of a bare ITO electrode, while GO exhibits an insulating character. Cycling for 20 times did not alter the electrochemical response as seen in Figure 4B, indicating a highly stable graphene/dopamine- $N_3$  assembly. This high stability might result from the way reduced graphene is functionalized with dopamine- $N_3$ . During the reduction of graphene, oxide dopamine- $N_3$  acts as reducing agent. The ortho-quinol structure is most likely oxidized during this process to quinone intermediates, which might bind covalently to graphene or to each other, explaining the strong stability. This behavior is in contrast to graphene/tetrathiafulvalene (TTF) nanocomposites formed in a similar manner.<sup>45</sup> Chemical oxidation of TTF to  $TTF^{2+}$  using an aqueous solution of  $Fe(ClO_4)_3$  expelled the charged molecule from the graphene nanosheets, which could be recaptured by immersion in neutral TTF solution.

Figure 5 displays the anodic scan of an ITO electrode coated with the graphene/dopamine- $N_3$  composite material in KCl (0.1M)/water. The presence of redox peaks ( $E_p = 0.80$  and  $1.17\text{ V}$  vs Ag/AgCl) are observed, corresponding to the oxidation of dopamine- $N_3$ . The reduction of the oxidized species is found at  $E_p = -0.01$  and  $-0.23\text{ V}$  vs Ag/AgCl. The CV is comparable with that of the dopamine- $N_3$  derivative in solution recorded on ITO (inset in Figure 5).

Tapping mode AFM imaging was used to estimate the thicknesses of the GO nanosheets before and after reduction.



**Figure 4.** (A) Scanning electron microscopy image of a graphene/dopamine- $N_3$  film deposited onto Si wafer by drop casting; (B) cyclic voltammograms of ITO (black), ITO/GO (blue), and ITO/graphene/dopamine- $N_3$  (red) in 5 mM  $Ru(NH_3)_6/0.1$  M KCl; scan rate = 50 mV/s.



**Figure 5.** Cyclic voltammograms of the ITO/graphene/dopamine- $N_3$  electrode in 0.1 M KCl aqueous solution, scan rate 50 mV/s; inset: CV of 10 mM dopamine- $N_3$  solution recorded on ITO.

The thickness of the sheets, measured from the line profile as the difference in height between the mica substrate and the sheet, is  $\sim 0.6$ – $0.7$  nm for as-prepared GO. This value matches well with reported apparent thicknesses of graphene oxide, suggesting single-layered GO sheets. Indeed, such a height is comparable to that reported by Paredes et al. ( $\sim 1.0$  nm).<sup>40</sup> The average thickness of the graphene/dopamine- $N_3$  composite material is about 1 nm, which is a typical characteristic of functional-molecule-modified single-layer graphene.<sup>17</sup>

To check the reactivity of the azide function in the graphene/dopamine- $N_3$  composite, the latter was reacted with ethynylferrocene in a “click chemistry” approach using the copper(I)-catalyzed Huisgen 1,3-dipolar cycloaddition. The success of the “click” reaction was confirmed clearly by the disappearance of the characteristic  $N_3$  vibration band at  $2103\text{ cm}^{-1}$  in the FTIR spectrum (data not shown).

Moreover, the successful incorporation of ferrocene moieties on the graphene/dopamine- $N_3$  was further confirmed by XPS analysis (Figure 6). The high resolution N 1s scan shows the nitrogen atoms for the triazole ring at about 400.7 eV (C–N) and 402.1 eV (N=N) together with the NH–C=O at 401.2 eV (Figure 6A). The high resolution XPS scan of the Fe 2p region demonstrates the presence of the ferrocene moieties (Figure 6B). The Fe  $2p_{3/2}$  and  $2p_{1/2}$  peaks occur at 711.7 and 725.6 eV, respectively. This clearly indicates that the Fe moiety

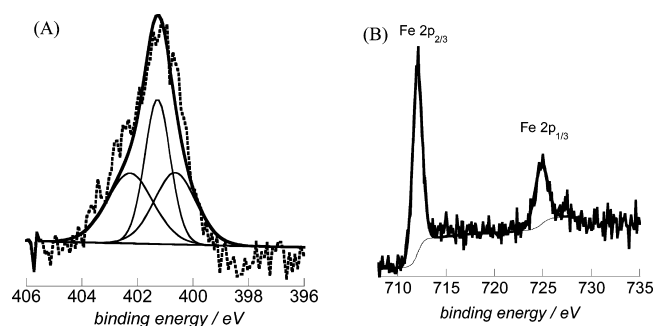


**Figure 6.** (A) N 1s and (B) Fe 2p high resolution XPS spectra of ITO/graphene/dopamine- $N_3$  interfaces after “clicking” of ethynylferrocene.

exists mainly in its (III) oxidation state, in agreement with previously reported results on ferrocene groups anchored onto diamond<sup>41</sup> and hydrogen-terminated silicon surfaces.<sup>42,43</sup>

The ferrocene-modified interface was additionally probed by CV in an aqueous solution containing 0.1 M KCl (Figure 7A).

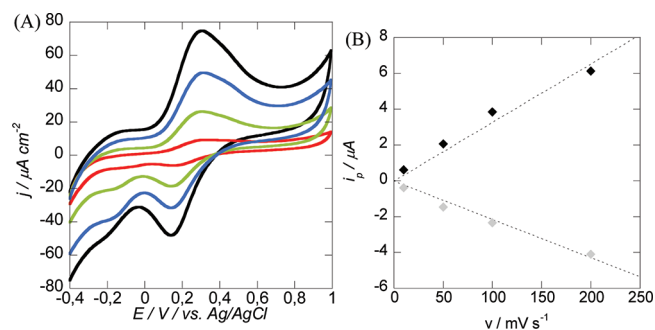


**Figure 7.** (A) CV of ITO/graphene/dopamine- $N_3$  interface after “clicking” ethynylferrocene; solution at different scan rates: 10 mV/s (red), 50 mV/s (green), 100 mV/s (blue), 200 mV/s (black); solution: KCl (0.1 M)/water, (B) change of anodic (■) and cathodic (□) peak current with scan rate.

The bound ferrocene moiety shows a redox potential of  $E^0 = 0.22$  V vs Ag/AgCl, being slightly lower than that found on gold ( $E^0 = 0.33$ – $0.46$  V vs Ag/AgCl).<sup>44</sup> Analysis of the change in the peak currents as a function of scan rates allows the assessment that the ferrocene moieties are surface linked. Figure 7B indicates that the anodic and cathodic peak currents scale linearly with the scan rate  $\nu$  rather than with  $\nu^{1/2}$ , suggesting a surface redox process. The ferrocene surface

coverage was calculated by integrating the anodic peak area according to  $\Gamma = Q_A/nFA$  where  $F$  is the Faraday constant,  $n$  the number of electrons exchanged ( $n = 1$ ), and  $A$  the surface area ( $A = 0.2 \text{ cm}^2$ ). A surface coverage of  $\Gamma = 4.09 \times 10^{14}$  molecules per  $\text{cm}^{-2}$  is obtained. This is in accordance with surface coverage obtained on boron-doped diamond interfaces using “click” chemistry.<sup>41</sup>

#### 4. CONCLUSION

This study demonstrated that dopamine induces simultaneous reduction of graphene oxide to graphene at room temperature under sonication and its functionalization. Using azide-terminated dopamine, functional graphene/dopamine- $\text{N}_3$  composite films can be easily formed in one step. The azide-functional groups can be readily reacted with alkynyl-terminated molecules in a “click chemistry” approach using the copper(I)-catalyzed Huisgen 1,3-dipolar cycloaddition. This approach opens new perspectives not only for the reduction of graphene oxide under mild conditions but also for a wide range of opportunities in graphene composite and sensor chemistry. The possibility to “click” different alkynyl-terminated glycans and glycan clusters to the graphene/dopamine- $\text{N}_3$  films is currently under investigation.

#### AUTHOR INFORMATION

##### Corresponding Author

\*E-mail: sabine.szunerits@iri.univ-lille1.fr.

#### ACKNOWLEDGMENTS

I.K. thanks the International PhD Projects Programme of the Foundation for Polish Science, cofinanced from European Regional Development Fund within Innovative Economy Operational Programme “Grants for Innovation”.

#### REFERENCES

- (1) Novoselov, K. S.; Geim, A. K.; Morozov, S. V.; Jiang, D.; Zhang, Y.; Dubonos, S. V.; Grigorieva, I. V.; Firsov, A. A. *Science* **2004**, *306*, 666–669.
- (2) Allen, M. J.; Tung, V. C.; Kaner, R. B. *Chem. Rev.* **2009**, *110*, 132.
- (3) Shao, Y.; Wang, J.; Wu, H.; Liu, J.; Aksay, I. A.; Lin, Y. *Electroanalysis* **2010**, *22*, 1027.
- (4) Li, L. X.; Zhang, G. Y.; Bai, X. D.; Sun, X. M.; Wang, X. R.; Wang, E.; Dai, H. J. *Science* **2008**, *319*, 1229.
- (5) Schedin, F.; Geim, A. K.; Morozov, S. V.; Hill, E. W.; Blake, P.; Katsnelson, M. I.; Novoselov, K. S. *Nat. Mater.* **2007**, *6*, 652.
- (6) Yang, S.-Y.; Chang, K.-H.; Tien, H.-W.; Lee, Y.-F.; Li, S.-M.; Wang, Y.-S.; Wang, J.-Y.; Ma, C.-C. M.; Hu, C.-C. *J. Mater. Chem.* **2011**, *21*, 2374.
- (7) Daton, A.; Radmilovic, V.; Lee, Z. H.; Phillips, J.; Frenklach, M. *Nano Lett.* **2008**, *8*, 2012.
- (8) Li, D.; Muller, M. B.; Gilje, S.; Kaner, R. B.; Wallace, G. G. *Nat. Nanotechnol.* **2008**, *3*, 101.
- (9) Paredes, J. I.; Villar-Rodil, S.; Fernandez-Merino, M. J.; Guardia, L.; Martinez-Alonso, A.; Tascon, J. M. D. *J. Mater. Chem.* **2011**, *21*, 298.
- (10) Lomeda, J. R.; Doyle, C. D.; Kosynki, D. V.; Hwang, W.-F.; Tour, J. M. J. *Am. Chem. Soc.* **2008**, *130*, 16201.
- (11) Wang, H.-X.; Zhou, K.-G.; Xie, Y.-L.; Zeng, J.; Chai, N.-N.; Li, J.; Zhang, H.-L. *Chem. Commun.* **2011**, *47*, 5747.
- (12) Avinash, M. B.; Subrahmanyam, K. S.; Sundarayya, Y.; Govindaraju, T. *Nanoscale* **2010**, *2*, 1762.
- (13) Dong, X.; Shi, Y.; Zhao, Y.; Chen, D.; Ye, J.; Yao, Y.; Gao, F.; Ni, Z.; Yu, T.; Shen, Z.; Huang, Y.; Chen, P.; Li, L.-J. *Phys. Rev. Lett.* **2009**, *102*, 135501.
- (14) Lee, D.-W.; Kim, T.; Lee, M. *Chem. Commun.* **2011**, *47*, 8259.
- (15) Chen, Q.; Wei, W.; Lin, J.-M. *Biosens. Bioelectron.* **2011**, *26*, 4497.
- (16) Varhese, N.; Ghosh, A.; Voggu, R.; Gosh, S.; Rao, C. N. R. *J. Phys. Chem. C* **2009**, *113*, 16855.
- (17) Rao, C. N. R.; Sood, A. K.; Subrahmanyam, K. S.; Govindaraj, A. *Angew. Chem., Int. Ed.* **2009**, *48*, 7752.
- (18) Xu, L. Q.; Yang, W. J.; Neoh, K.-G.; Kang, E.-T.; Fu, G. D. *Macromolecules* **2010**, *43*, 8336.
- (19) Lee, H.; Dellatore, S. M.; Miller, W. M.; Messersmith, P. B. *Science* **2007**, *318*, 426.
- (20) Zurcher, S.; Wackerlin, D.; Bethuel, Y.; Malisova, B.; Textor, M.; Tosatti, D.; Gademann, K. *J. Am. Chem. Soc.* **2006**, *128*, 1064.
- (21) Watson, M. A.; Lyskawa, J.; Zobrist, C.; Fournier, D.; Jimenez, M.; Traisnel, M.; Gegembre, L.; Woisel, P. *Langmuir* **2010**, *26*, 15920.
- (22) Alwarappan, S.; Erdem, A.; Liu, C.; Li, C.-Z. *J. Phys. Chem. C* **2009**, *113*, 8853.
- (23) Shang, N. G.; Papakonstantinou, P.; McMullan, M.; Chu, M.; Stamboulis, A.; Potenza, A.; Dhesi, S. S.; Marchetto, H. *Adv. Funct. Mater.* **2008**, *18*, 3506.
- (24) Wang, Y.; Li, Y.; Tang, L.; Lu, J.; Li, J. *Electrochem. Commun.* **2009**, *11*, 889.
- (25) Kolb, H. C.; Finn, M. G.; Sharpless, K. B. *Ang. Chem. Int. Ed.* **2001**, *40*, 2004.
- (26) Manova, R.; Van Beek, T. A.; Zuilhof, H. *Angew. Chem., Int. Ed.* **2001**, *50*, 5428.
- (27) Jin, Z.; McNicolas, T. P.; Shih, C.-J.; Wang, Q. H.; Paulus, G. L. C.; Hilmer, A. J.; Shimizu, S.; Strano, M. S. *Chem. Mater.* **2011**, *23*, 3362.
- (28) Das, M. R.; Sarma, R. K.; Saikia, R.; Kale, V. S.; Shelke, M. V.; Sengupta, P. *Colloids Surf., B* **2011**, *83*, 16.
- (29) Barras, A.; Szunerits, S.; Marcon, L.; Monfilliette-Dupont, N.; Boukherroub, R. *Langmuir* **2010**, *26*, 13168.
- (30) Fu, Y. C.; Li, P. H.; Xie, J. Q.; Xu, X. H.; Lei, L. H.; Chen, C.; Zou, C.; Deng, W.; Yao, S. Z. *Adv. Funct. Mater.* **2009**, *19*, 1784.
- (31) Fei, B.; Qian, B. T.; Yang, Z. Y.; Wang, R. H.; Liu, W. C.; Mak, C. L.; Xin, J. H. *Carbon* **2008**, *46*, 1795.
- (32) Lia, K.-H.; Mittal, A.; Bose, S.; Leighton, C.; Myhoyan, K. A.; Macosko, C. W. *ACS Nano* **2011**, *5*, 1253.
- (33) Fellahi, O.; Das, M. R.; Coffinier, Y.; Szunerits, S.; Hadjersi, T.; Maamache, M.; Boukherroub, R. *Nanoscale* **2011**, *3*, 4662.
- (34) Stankovich, S.; Dikin, D. A.; Piner, R. D.; Kohlhaas, K. A.; Kleinhammes, A.; Jia, Y.; Wu, Y.; Nguyen, S. T.; Ruoff, R. S. *Carbon* **2007**, *45*, 1558–1565.
- (35) Szunerits, S.; Niedziolka-Jonsson, J.; Boukherroub, R.; Woisel, P.; Baumann, J.-S.; Siriwardena, A. *Anal. Chem.* **2010**, *82*, 8203.
- (36) Barka, F.; Niedziolka-Jonsson, J.; Castel, X.; Akjouj, A.; Pennec, Y.; Djafari-Rouhani, B.; Woisel, P.; Bezzi, N.; Boukherroub, R.; Szunerits, S. *J. Mater. Chem.* **2011**, *21*, 3006.
- (37) Zhang, J. L.; Yang, H. J.; Shen, G. X.; Cheng, P.; Zhang, J. Y.; Guo, S. W. *Chem. Commun.* **2010**, *46*, 1112.
- (38) McCrerry, R. L. *Chem. Rev.* **2008**, *108*, 2646.
- (39) Tang, L.; Wang, Y.; Li, Y.; Feng, H.; Lu, J.; Li, J. *Adv. Funct. Mater.* **2009**, *19*, 2782.
- (40) Paredes, J. I.; Villar-Rodil, S.; Solis-Fernandez, P.; Martinez-Alonso, A.; Tascon, J. M. D. *Langmuir* **2009**, *25*, 5957.
- (41) Das, M. R.; Wang, M.; Szunerits, S.; Gegembre, L.; Boukherroub, R. *Chem. Commun.* **2009**, 2753.
- (42) Rohde, R. D.; Agnew, H. D.; Yeo, W.-S.; Bailey, R. C.; Heath, J. R. *J. Am. Chem. Soc.* **2006**, *128*, 9518.
- (43) Ciampi, S.; Bocking, T.; Kilian, K. A.; James, M.; Harper, J. B.; Gooding, J. J. *Langmuir* **2007**, *23*, 9320.
- (44) Collman, J. P.; Devaraj, N. K.; Chidsey, C. E. D. *Langmuir* **2004**, *20*, 1051.
- (45) Kaminska, I.; Das, M. R.; Coffinier, Y.; Niedziolka-Jonsson, J.; Woisel, P.; Opallo, M.; Szunerits, S.; Boukherroub, R. *Chem. Commun.* **2012**, *48*, 1221.